

# Green corrosion inhibitor from seed extract of *Areca catechu* for mild steel in hydrochloric acid medium

K. P. Vinod Kumar · M. Sankara Narayanan Pillai ·  
G. Rexin Thusnavis

Received: 5 November 2010 / Accepted: 9 March 2011 / Published online: 22 March 2011  
© Springer Science+Business Media, LLC 2011

**Abstract** The adsorption and corrosion inhibition effect of acid extract of the seeds of *Areca catechu* on mild steel in hydrochloric acid medium were analyzed. Inhibition efficiency and thermodynamic parameters such as energy of activation for corrosion reaction of mild steel ( $E$ ), heat of adsorption of the inhibitor on the metal surface ( $Q$ ), change in entropy ( $\Delta S$ ), and change in free energy ( $\Delta G$ ) were obtained using weight-loss data. The nature of adsorption of the inhibitor on the metal surface was verified by plotting Temkin's adsorption isotherm. Electrochemical parameters were obtained by AC impedance and Tafel polarization studies. Infrared (IR) spectra and scanning electron microscope techniques were also employed to examine the mechanism of corrosion inhibition property. All the results obtained were encouraging and hence bring to light a new alternate, eco-friendly material for the corrosion inhibition of mild steel in acid medium.

## Introduction

Mild steel, an alloy of choice for industries due to its low cost and easy fabrication, undergoes corrosion in adverse environmental conditions. The elimination of detrimental rust and scale in several industrial processes is carried out by pickling using acid solutions especially hydrochloric acid. In petrochemical industries, corrosion of mild steel is a major distress due to the severe attack by hydrochloric acid when used as a cleaning agent, through chemical reactions. Petrochemical industries including refineries utilize different film forming organic corrosion inhibitors to prevent electrochemical corrosion [1–3]. Even though there are several techniques to minimize corrosion in various industries, the only way to do so in petrochemical industries is by adding small amount of inhibitor to hydrochloric acid solution.

The strict environmental regulations and increasing ecological awareness has indeed shifted the attention of researchers to focus on eco-friendly materials and processes. Natural products extracted from plant sources as well as some nontoxic organic compounds, which contain polar functions with nitrogen, oxygen and/or sulfur atoms in their molecules have been effectively used as inhibitors in many corrosion systems [4–11]. The effectiveness of corrosion inhibition by *Uncaria gambir* [12] and *Strychnos nux-vomica* [13] are also proved. The gum extract obtained from *Raphia hookeri* [14] is reported to be an effective corrosion inhibitor in acid medium. *Piper guinensis* [15], *Solanum tuberosum* [16], and *Parthenium hystophrous* L. [17] have also been analyzed for corrosion inhibition properties. Acid extract of the leaves of *Citrus aurantiifolia* [18] and *Ficus exasperata* [19] have also been examined for its inhibitory effect on mild steel corrosion. The corrosion inhibitive effect of *Eclipta alba* [20] and *Phyllanthus amarus* [21] are also investigated and proved to be

---

K. P. Vinod Kumar (✉)

Department of Chemistry, University College of Engineering,  
Nagercoil, Anna University Tirunelveli, Nagercoil 629004,  
Tamil Nadu, India  
e-mail: nanjilvino@rediffmail.com

M. Sankara Narayanan Pillai

Department of Chemistry, Noorul Islam University, Kumaracoil,  
Nagercoil, Tamilnadu, India  
e-mail: msankars@yahoo.com

G. Rexin Thusnavis

Department of Chemistry, St. Xavier's Catholic College  
of Engineering, Chunkankadai, Nagercoil 629003,  
Tamil Nadu, India  
e-mail: grt\_rexin@yahoo.co.in



**Fig. 1** *A. catechu* seeds



**Fig. 2** *A. catechu* seed powder

successful. In this context, the corrosion inhibition effect of acid extract of the seeds (Figs. 1, 2) of *A. catechu* on mild steel in hydrochloric acid medium is examined.

*A. catechu*, colloquially known as “Betel nut” is a species of palm, which grows in tropical Pacific, Asia and parts of east Africa. It is a medium sized tree, which grows straight to 20 m height. This tree is grown in India, Malaysia, Taiwan, and many other Asian countries for mainly its seed and timber value.

## Experimental

### Preparation of extract

50 g of air dried *A. catechu* seed powder was mixed with 100 mL of 5% HCl and refluxed for 1 h and the extract was

filtered off using Whatman No. 1 filter paper. This filtrate is then subjected to vacuum distillation to get the dry solid inhibitor.

### Preparation of MS specimen

Mild steel (MS) specimens of composition C = 0.01%, Mn = 0.034%, P = 0.08%, and Fe = 99.51% with the size of 4.0 × 2.0 × 0.19 cm were used for weight loss study. Mild steel powder was used for infrared studies. MS specimens with an exposed area of 1 cm<sup>2</sup> (remaining area covered with Teflon holder) were used for electrochemical studies. “SEM” studies were carried out with MS specimens fabricated exactly to 1 cm<sup>2</sup>. The specimens used were polished mechanically followed by different grades of emery paper and then degreased with trichloroethylene. Throughout the studies, analytic grade HCl and double distilled water were used.

### Preparation of corrosive environment

The corrosive environment of 5% HCl solution was prepared using HCl and double distilled water. From this stock solution, 100 mL each of test solutions with different concentrations of inhibitors were prepared.

### Weight loss and thermodynamic studies

Previously polished and degreased MS specimens of size 4.0 × 2.0 × 0.19 cm were used for the weight loss study. Already weighed MS plates were separately immersed in 100 mL of the test solutions for 1 h. These test solutions contain 100, 200, 300, 400, 500 ppm of the plant extract. After the specified time, the MS specimens were washed immediately with double distilled water, dried, and weighed again using Schimadzu AUX220 balance. The same experiment was carried out at four different temperatures of 303, 308, 313, and 318 K, respectively. From the measured weight loss data, the inhibition efficiency (IE) was calculated using the formula

$$IE\% = \frac{(W_0 - W_i)}{W_0} \times 100$$

where  $W_i$  and  $W_0$  are the weight loss values in the presence and absence of the inhibitor.

The corrosion rate (CR) in mmpy was calculated using the following formula

$$CR = \frac{87.6 \times W}{DAT}$$

where  $W$  is weight loss in mg,  $D$  is the density of mild steel,  $A$  is the area of exposure in (cm<sup>2</sup>), and ‘ $T$ ’ is the time in hours [17].

$E$ , energy of activation was obtained using the formula

$$\log \frac{CR_2}{CR_1} = \frac{E}{2.303R} \times \left[ \frac{1}{T_1} - \frac{1}{T_2} \right]$$

where  $CR_1$  and  $CR_2$  are the corrosion rates at temperatures  $T_1$  and  $T_2$ , respectively, [22, 23].

$Q$ , the heat of adsorption was obtained by plotting  $\log \theta/1 - \theta$  against  $1/T$  where  $\theta$  is the fraction of the metal surface covered by the inhibitor at temperature  $T$ , respectively. A negative slope was obtained that was equivalent to  $-Q/2.303R$  from which  $Q$  was calculated. The entropy change ( $\Delta S$ ) for the adsorption process is obtained by plotting a graph between  $\log CR/T$  against  $1/T$ . The obtained intercept is equivalent to  $\log(R/Nh) + (\Delta S/2.303R)$  from which,  $\Delta S$  is calculated ( $R$  is the gas constant,  $N$  is the Avogadro number and  $h$  is the Planck's constant) [24].

The free energy change,  $\Delta G$  for the adsorption [15] was calculated using the formula  $\Delta G = -2.303RT \log 55.5K$ , where  $K = (\theta/1 - \theta)/C$

#### Polarization and impedance studies

The electrochemical parameters were studied in HCl medium and also with different concentrations of natural inhibitor. Impedance measurements were carried out in the frequency Range of 10 kHz to 10 mHz [25]. Tafel polarization studies were carried out potentiodynamically. In this set up, Pt, calomel and MS specimen were used as auxiliary, reference and working electrodes, respectively. Potentiodynamic polarization studies were carried out at a sweep rate of 1 mV/sec.

Both impedance and polarization studies were carried out using Solartron model 1280B electrochemical measurement unit.

#### Scanning electron microscope studies

Mild steel specimens were immersed in a corrosive environment of 5% HCl having an optimum concentration (500 ppm) of the extract for 1 h. The specimens were dried

and scanned at 10 K using Hitachi S-3000H model Scanning electron microscope.

#### Infrared spectroscopy studies

FTIR spectrum was recorded with a frequency ranging from 4,000 to 400  $\text{cm}^{-1}$  for the saturated solution of the extract prepared in 5% HCl and finely powdered sample immersed in a saturated solution of the extract for 4 h using Bruker FTIR model-Tensor27.

## Results and discussion

The major constituents of the nut are polyphenols (flavonols and tannins), alkaloids (Arecoline, Arecaidine, Guvacoline, and Guvacine), carbohydrates, fats, proteins, crude fiber, and mineral matters [26].

#### Weight loss analysis

The weight loss values and inhibition efficiency (IE) at four different temperatures are given in Table 1. From the table it is clear that, increase in inhibitor concentration increases the IE. The inhibition efficiency is found to be more or less the same with rise in temperature. However, it is obvious from Table 1 that the weight loss increase is significant as the temperature is raised. This reflects the high magnitude of corrosion at elevated temperature. A decrease in IE is observed when the exposure time is increased above 1 h as shown in Fig. 3.

#### Thermodynamic studies

Even at the lowest concentration, the *A. catechu* extract is able to bring down the corrosion rate substantially (Table 2). The corrosion rate is found to decrease tremendously even at 100 ppm inhibitor concentration and found to decrease steadily at higher inhibitor strengths irrespective of the temperature. The  $E$  values for the corrosion reaction are found to be higher in the presence of the

**Table 1** Weight loss data

Concentration of the inhibitor (ppm)	Weight loss (g)				Inhibition efficiency (%)			
	303 K	308 K	313 K	318 K	303 K	308 K	313 K	318 K
0	0.0594	0.0648	0.0662	0.0755	–	–	–	–
100	0.0036	0.0041	0.0044	0.0053	93.94	93.67	93.35	92.98
200	0.0027	0.0031	0.0034	0.0040	95.45	95.22	94.86	94.70
300	0.0022	0.0025	0.0028	0.0034	96.29	96.14	95.77	95.49
400	0.0020	0.0022	0.0023	0.0028	96.63	96.60	96.52	96.29
500	0.0018	0.0020	0.0021	0.0025	96.97	96.91	96.83	96.68

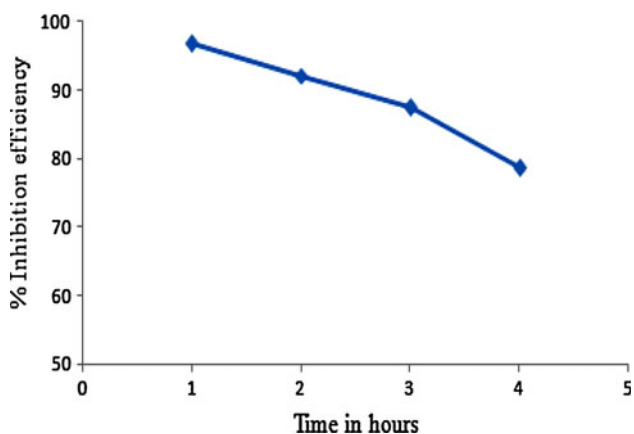


Fig. 3 Inhibition efficiency for 500 ppm versus time

inhibitor for all temperature ranges. This indicates the requirement of more energy for the oxidation reaction, and hence prevents corrosion.

The  $Q$  values are found to be very low for different concentrations of the inhibitor as given in Table 3. As the concentration of the inhibitor increases, adsorption also increases, releasing more quantity of heat which is evident from the  $Q$  values given in the Table 3. The high negative  $\Delta S$  value reveals increased adsorption of the inhibitor on the MS surface. The free energy change value for this adsorption process is around  $-14$  kJ/mol. The adsorption of different organic compounds of the extract on the metal surface is spontaneous, which is revealed by the negative-free energy values. Gibbs free energy values between  $-49$

and  $-58$  kJ/mol are indicative of chemisorptions [8]. Hence in the present case, the low free-energy change values further confirm that the adsorption is physical in nature.

The inhibition efficiency is found to increase linearly with the increase of the inhibitor concentration. Finally, at higher concentrations it reaches a limiting value irrespective of the inhibition process carried out at temperature variance as observed in Fig. 4. From the graph plotted between corrosion rate and concentration of inhibitor, it is revealed that the corrosion rate reaches almost a constant value at higher concentrations of the inhibitor. The trend continued even at elevated temperatures as noted from the Fig. 5.

Adsorption studies

A straight-line plot (Fig. 6) is obtained when a graph was drawn between  $\log C$  and  $\theta$  (where  $C$  is the concentration of the inhibitor). The plot is also found to fit exactly Temkin adsorption isotherm, which is mathematically given by

$$\theta = a + b \log C$$

where  $a$  and  $b$  are intercept and slope, respectively. This isotherm reveals the increased adsorption of the inhibitor on the MS surface with increase in its concentration and thus the increased protection. From the graph it is clear that the level of adsorption of the inhibitor on the metal surface increases with increase in inhibitor concentration [18].

Table 2 Corrosion rate and energy of activation data

Concentration of the inhibitor (ppm)	Corrosion rate (mmpy)				$E$ in KJ/mol for the range (K)		
	303 K	308 K	313 K	318 K	303–308	308–313	313–318
0	36.26	39.56	40.41	46.09	13.50	3.43	21.78
100	2.19	2.50	2.69	3.24	20.54	11.73	30.82
200	1.65	1.89	2.08	2.44	21.04	15.35	26.43
300	1.34	1.53	1.71	2.08	20.58	17.82	32.46
400	1.22	1.34	1.40	1.71	14.54	7.01	33.15
500	1.09	1.22	1.28	1.53	17.47	7.71	29.56

Table 3 Heat of corrosion reaction and change in free energy data

Concentration of the inhibitor (ppm)	$\Delta S$ in (J/mol)	$Q$ in (KJ/mol)	$\Delta G$ in (KJ/mol)			
			303 K	308 K	313 K	318 K
100	-252.66	-8.48	-15.28	-15.41	-15.53	-15.62
200	-256.09	-9.13	-14.29	-14.39	-14.43	-14.58
300	-257.97	-11.45	-13.81	-13.93	-13.91	-13.96
400	-252.55	-5.11	-13.34	-13.53	-13.69	-13.73
500	-255.61	-4.96	-13.05	-13.21	-13.36	-13.45

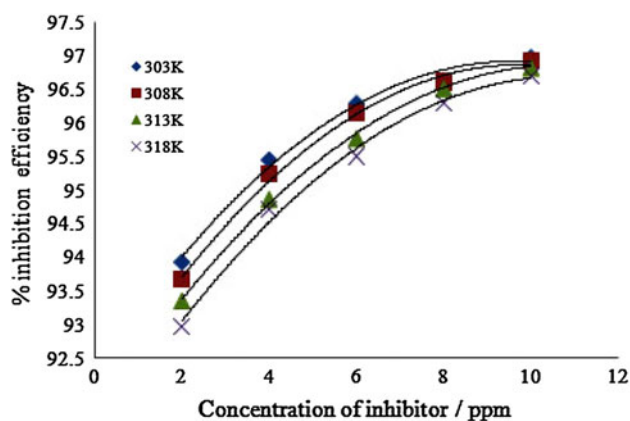


Fig. 4 Concentration versus inhibition efficiency

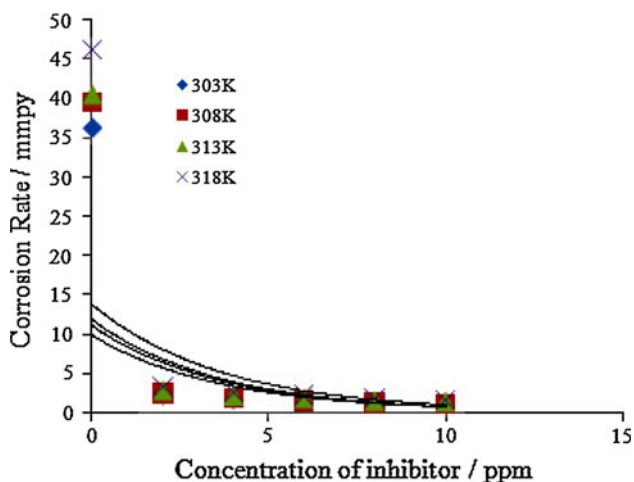


Fig. 5 Corrosion rate versus concentration of inhibitor

#### Polarization and impedance analysis

The values obtained from electrochemical measurements such as open circuit potential (OCP), corrosion potential ( $E_{\text{corr}}$ ), corrosion current ( $I_{\text{corr}}$ ), anodic and cathodic Tafel slopes ( $b_a$  and  $b_c$ ), charge transfer resistance ( $R_{\text{ct}}$ ), double layer capacitance ( $C_{\text{dl}}$ ), and IE are given in Table 4. The observed  $E_{\text{corr}}$  values do not change in a regular manner from the blank value. This indicates that the inhibitor

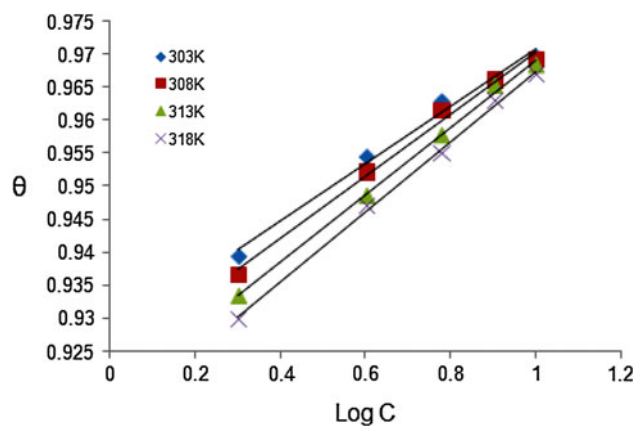


Fig. 6 Adsorption isotherm

works through mixed mode of inhibition. It is obvious from Fig. 7, that Tafel curves are shifted markedly to lower corrosion current density as the inhibitor concentration is raised. The  $I_{\text{corr}}$  values decrease steadily from the blank value with increase in inhibitor concentration. This decrease in  $I_{\text{corr}}$  is an indication of decrease in corrosion reaction, since corrosion current is proportional to the magnitude of corrosion reaction. The  $b_a$  and  $b_c$  values change upon addition of the inhibitor from the blank, which means the extract molecules are adsorbed both on anodic and cathodic sites. This results in the inhibition of both anodic metal dissolution and cathodic reduction reactions of hydrogen ion of the acid. Generally the inhibitor acts as a mixed type, but predominantly retards the cathodic reaction [25].

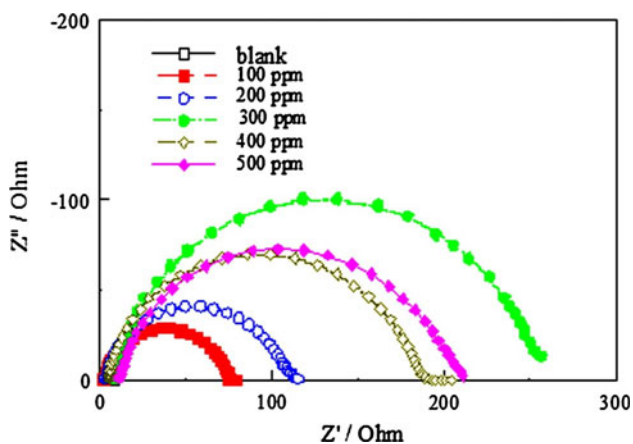
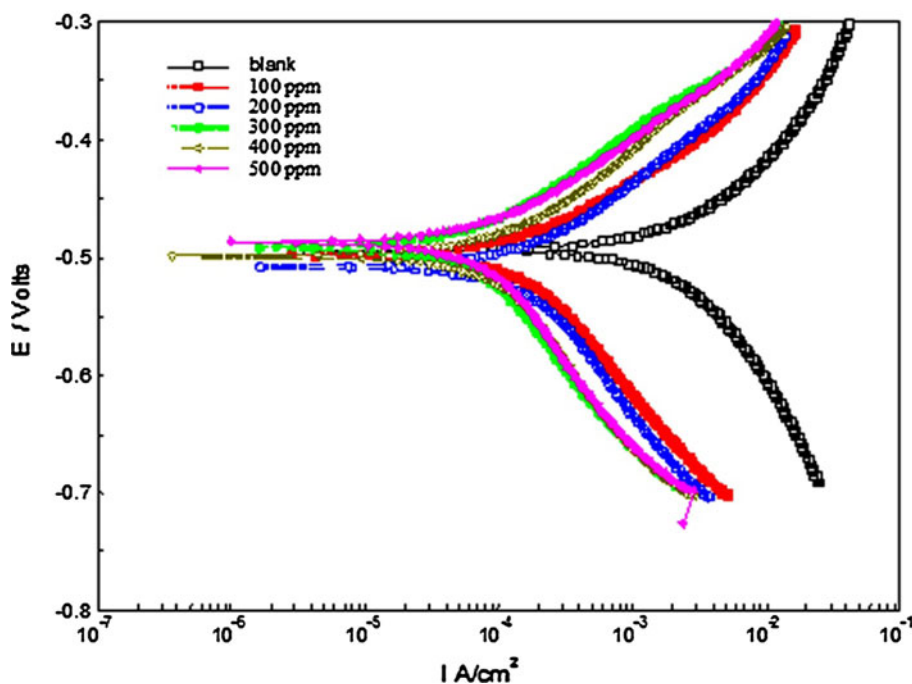
The impedance spectra (Fig. 8) exhibit a single semicircle for a particular concentration, and the diameter of semicircle increases with increase in inhibitor concentration. The single semicircle indicates that the charge transfer takes place at electrode/solution interface, and the corrosion reaction of MS is controlled by the charge transfer process. These impedance diagrams are not perfect semicircles, which are related to the frequency dispersion as a result of the roughness and inhomogeneity of the MS electrode surface. Moreover, the impedance response of MS in HCl medium alone has changed significantly after

Table 4 Electrochemical parameters of corrosion inhibition by *A. catechu* extract

Concentration of the inhibitor (ppm)	OCP (mV)	$E_{\text{corr}}$ versus SCE (mV)	$I_{\text{corr}}$ ( $\mu\text{A}$ )	$b_a$ (mV/dec)	$b_c$ (mV/dec)	$R_{\text{ct}}$ (Ohm/ $\text{cm}^2$ )	$C_{\text{dl}}$ ( $\mu\text{A}/\text{cm}^2$ )	%IE
0	-0.5151	-0.4939	$26.78 \times 10^{-4}$	150.9	226.1	5.804	$6.0785 \times 10^{-5}$	-
100	-0.5	-0.4974	$1.75 \times 10^{-4}$	84.8	139.3	73.99	$3.79 \times 10^{-5}$	93.48
200	-0.5215	-0.5084	$1.68 \times 10^{-4}$	89.7	151.7	109.06	$3.39 \times 10^{-5}$	93.72
300	-0.5053	-0.4081	$1.05 \times 10^{-4}$	92.3	161.3	183.05	$3.15 \times 10^{-5}$	96.07
400	-0.5056	-0.4867	$8.18 \times 10^{-5}$	79.2	159.1	197.57	$3.33 \times 10^{-5}$	96.94
500	-0.5049	-0.4914	$6.4 \times 10^{-5}$	77.1	148.4	260.83	$3.69 \times 10^{-5}$	97.61



**Fig. 7** Tafel polarization plots for the corrosion inhibition effect of the seed extract of *A. Catechu* on mild steel



**Fig. 8** Impedance spectra for the corrosion inhibition effect of the seed extract of *A. Catechu* on mild steel

addition of the inhibitor. The value of  $C_{dl}$  (Table 4) decrease from the blank value as the concentration of the inhibitor is increased, which confirms the increased level of adsorption of the inhibitor on the metal surface [25]. The adsorption may be due to the hetero atoms such as ‘N’ and ‘O’, which are present in the organic constituents of the extract on the metal surface. The  $R_{ct}$  values increase from the blank value as the inhibitor concentration is raised. This indicates the resistance toward charge transfer reactions responsible for corrosion process. These observations clearly prove the dependence of inhibitor concentration on corrosion control. The inhibition efficiency obtained from weight loss and electrochemical measurements are in good agreement at all concentrations.

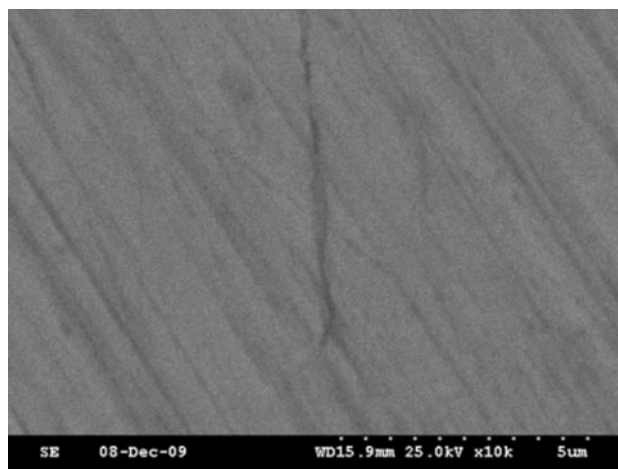


**Fig. 9** Polished mild steel surface

Scanning electron microscope results

The surface morphology of steel is examined by scanning electron microscopy. SEM photographs of the steel surface (Fig. 9) and metal surface without and with (500 ppm) inhibitor in hydrochloric acid media were recorded. The SEM photograph shows cracks on the surface of the metal (Fig. 10). But in the presence of inhibitor, these are minimized on the metal surface (Fig. 11). This is due to the formation of protective organic layer on the metal surface (Fig. 11) [27]. The relatively uneven surface when compared to MS surface is attributed to the adsorption of arecaidine and guvacoline present in the extract.

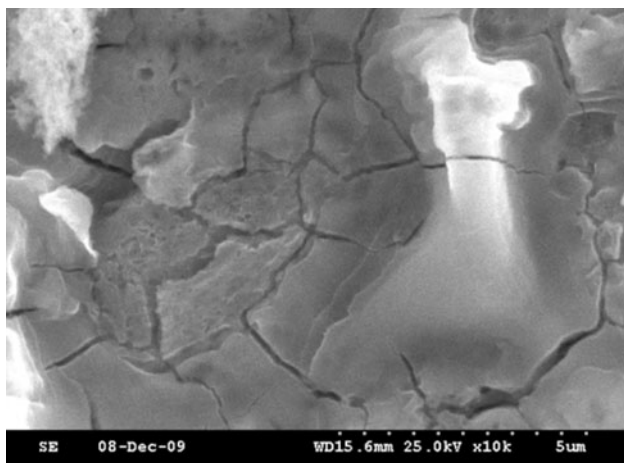


**Fig. 10** Mild steel exposed to 5% HCl alone

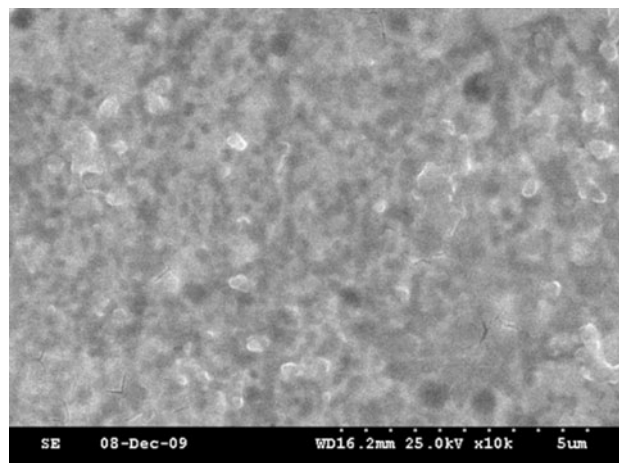


**Fig. 11** Mild steel sample exposed to 5% HCl having 500 ppm of inhibitor

### IR analysis

The infrared spectra of *A. catechu* extract and the product of adsorption between extract and MS powder are given in Figs. 12 and 13, respectively. From the spectra, it is observed that the OH stretching frequency of carboxylic acid is shifted from 3427.8 to 3421.1  $\text{cm}^{-1}$ . The carbonyl (C=O) group frequency has vanished from 1712.2  $\text{cm}^{-1}$  which is due to the interaction between the functional group and the metal. The C–O stretching frequency of carboxylic acid group is downshifted from 1062.5 to 1053.9  $\text{cm}^{-1}$ . The C=C stretching frequency is also changed from 1631.6 to 1633.3  $\text{cm}^{-1}$ . Tertiary amine group (C–N) frequency has also vanished from 1226.1  $\text{cm}^{-1}$ . These group frequency changes for the functional groups of

organic molecules of *A. catechu* extract confirm the adsorption on the metal surface, which is responsible for preventing corrosion.

### Conclusion

From the weight loss study, it is observed that the corrosion inhibition efficiency of *A. catechu* extract increases with the increase in inhibitor concentration and decrease as the temperature is increased. The adsorption isotherm plotted between  $\log C$  versus  $\theta$  clearly reveals the increased adsorption of inhibitor on the metal surface with the increase in concentration. The free energy change values

**Fig. 12** IR spectra of the *A. catechu* extract

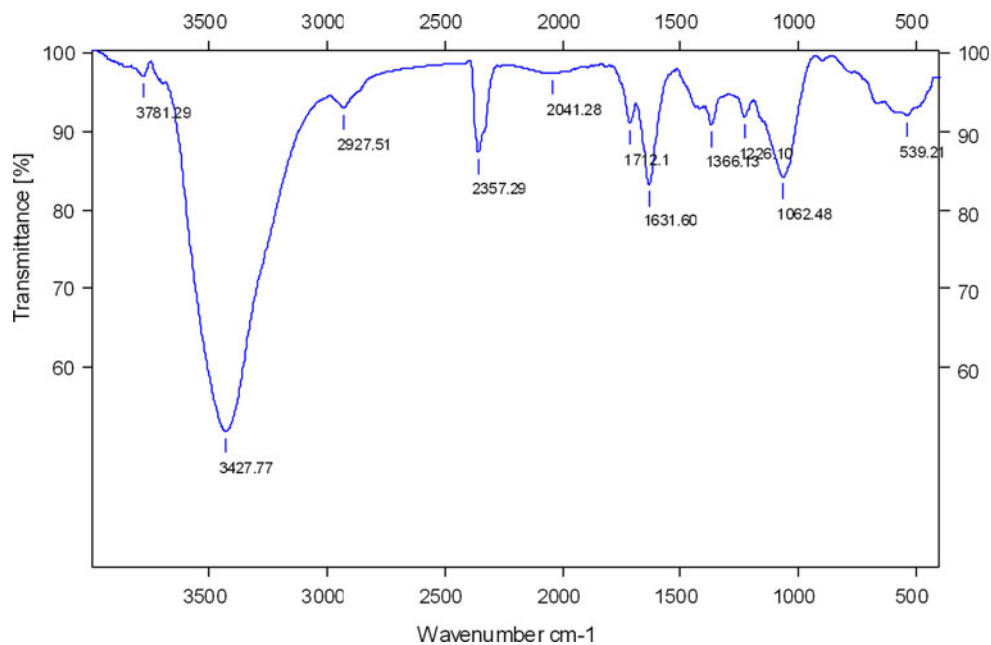
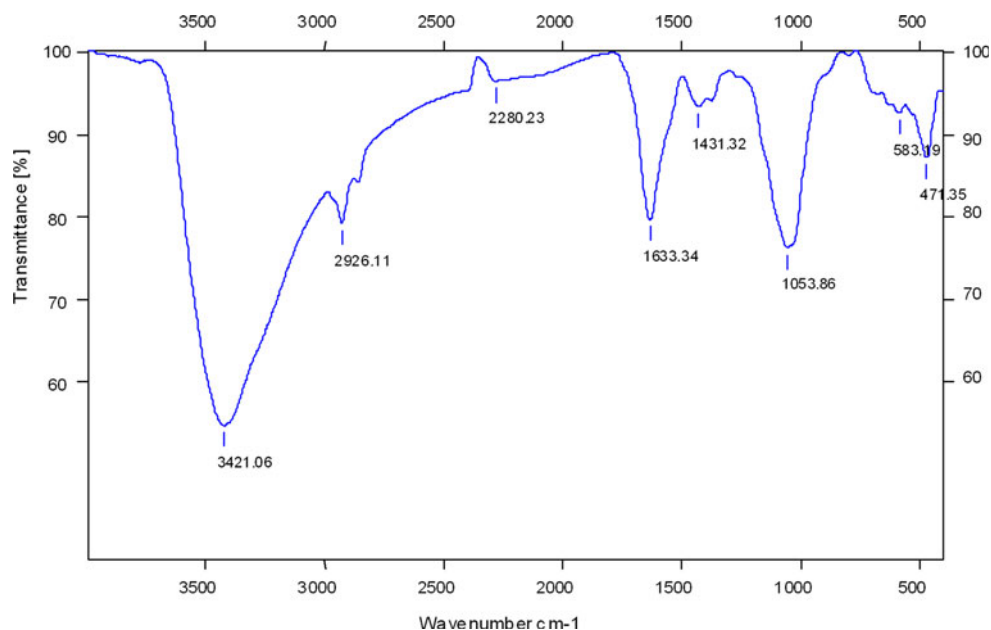


**Fig. 13** IR spectra of the reaction product between *A. catechu* extract and MS powder



predict the spontaneity of the adsorption process. The mixed mode of inhibition is indicated from the electrochemical parameters such as  $E_{\text{corr}}$ ,  $b_a$ , and  $b_c$ . IR spectral study indicates that the adsorption is through the lone pair of electrons present in the hetero atoms like N and O of the *A. catechu* extract. The SEM photographs obtained clearly predict the protective nature of the extract on mild steel. From the complete studies it is proved that, *A. catechu* extract can be used as an effective eco-friendly corrosion inhibitor for mild steel in HCl medium.

**Acknowledgement** The authors sincerely thank The Director, CECRI, Karaikudi for his kind permission to use lab facilities. Further, the authors are grateful to Dr. S. Muralidharan, Mr. Ravi Shankar, and Mrs. Nalini, CECRI, Karaikudi, Dr. M Shankara Narayana Pillai, Noorul Islam University, Nagercoil and Dr. S. Athimoolam, Anna University, Tirunelveli for rendering their immense support through discussions.

## References

- D'yakov VG, Shreider AV (1976) Chem Technol Fuels Oil 12(12):926
- Durnie W, Marco RD, Jefferson A, Kinsella B (1999) J Electrochem Soc 146(5):1751
- Ramachandran S, Tsai BL, Blanco M, Chen H, Tang YC, Goddard WA (1996) Langmuir 12(26):6419
- Lowmunkhong P, Ungtharak D, Sutthivaiyakit P (2010) Corros Sci 52:30
- Ogoko EC, Odoemelam SA, Ita BI, Eddy NO (2009) Port Electrochim Acta 27(6):713
- Amin MA, Abd El Rehim SS, El-Naggar MM, Abdel-Fatah Hesham TM (2009) J Mater Sci 44(23):6258. doi:10.1007/s10853-009-3856-2
- JJ FU, Li SN, Cao LH, Wang Y, Lu LD (2010) J Mater Sci 45(4):979. doi:10.1007/s10853-009-4028-0
- Singh MR, Bhrara K, Singh G (2008) Port Electrochim Acta 26(6):479
- Dubey AK, Singh G (2007) Port Electrochim Acta 25:221
- Eddy NO, Mamza PAP (2009) Port Electrochim Acta 27(4):443
- Ekanem UF, Umoren SA, Udousoro II, Udoh AP (2010) J Mater Sci 45(20):5558. doi:10.1007/s10853-010-4617-y
- Hussin MH, Kassim MJ (2010) J Phys Sci 21(1):1
- Raja PB, Sethuraman MG (2008) Mater Corros 60(1):22
- Umoren SA, Obot IB, Obi-Egbedi NO (2009) J Mater Sci 44:274. doi:10.1007/s10853-008-3045-8
- Ebenso EE, Eddy NO, Odiogenyi AO (2008) Afr J Pure Appl Chem 2(11):107
- Pandian, Raja PB, Sethuraman MG (2009) Iran J Chem Chem Engg 28(1):77
- Muhamath AliBM, Kulanthai Kannan (2009) J Appl Sci Environ Mgt 13:27
- Saratha R, Priya SV, Thilagavathy P (2009) e-J Chem 6(3):785
- Patel NS, Jauhari S, Mehta GN (2009) e-J Chem 6(S1):89
- Shyamalay M, Arulanantham A (2009) J Mater Sci Technol 25(5):633
- Okafor PC, Ikpi MI, Uwah IE, Ebenso EE, Ekpe UJ, Umoren SA (2008) Corros Sci 50(8):2310
- Das C, Gadiyar HS (1993) J Electrochem Soc India 42(4):225
- Sethuraman MG, Raja PB (2009) Pigment Resin Technol 38(1):33
- Singh AK, Quraishi MA (2010) Corros Sci 52:152
- Shanbhag AV, Venkatesha TV, Prabhu RA, Kalkhambkar RG, Kulkarni GM (2008) J Appl Electrochem 38:279
- World Health Organization (2004) IARC Monographs on the evaluation of carcinogenic risks to humans 85:44
- Prabhu RA, Venkatesha TV, Shanbhag AV (2009) J Iran Chem Soc 6(2):353